P-ISSN 2586-9000
E-ISSN 2586-9027
Homepage : https://tci-thaijo.org/index.php/SciTechAsia
Science & Technology Asia
Vol.27 No.2 April - June 2022
Page: [189-198]
Original research article

Bearing Capacity Factor for Spudcans in Anisotropic Clay Based on AUS Failure Criterion

Suraparb Keawsawasvong*

Department of Civil Engineering, Thammasat School of Engineering, Thammasat University, Pathum Thani 12120, Thailand

Received 24 January 2021; Received in revised form 22 April 2021
Accepted 29 April 2021; Available online 29 June 2022

ABSTRACT

New plastic solutions of spudcan foundations in anisotropic clay are presented in this paper. It is well known that natural clays exhibit some degree of strength anisotropy due to their deposition and sedimentation processes. Despite the important aspect of anisotropic clay, there is no existing solution for the bearing capacity of spudcans in anisotropic clay in the literature. An efficient numerical technique, namely the finite element limit analysis, is employed to derive the bearing capacity solutions of such foundation, where the Anisotropic Undrained Shear (AUS) failure criterion is associated with the computations. This failure criterion consists of three unequal undrained shear strengths obtained from the triaxial compression test, triaxial extension test, and direct simple shear test. In this paper, new solutions of the bearing capacity of spudcans in anisotropic clay are first-time derived based on two major dimensionless parameters, which are the cone apex angle and the undrained shear strength ratio obtained from the triaxial compression test and triaxial extension test. In addition, the failure mechanisms of the spudcans are examined and discussed to portray the effects of two major dimensionless parameters. The proposed solutions in this paper can be used as design charts for general design purposes of several offshore structures.

Keywords: Spudcan; Anisotropic Clay; Bearing Capacity; Finite Element Limit Analysis; Offshore Foundation

1. Introduction

A spudcan is one of the foundation systems that is commonly used as a base cone for supporting the load transferred from a mobile-drilling jack-up platform. This platform is widely used for most offshore drilling operations in water depths up to around 150 m. The spudcan is an axisymmetric footing with a conical shape. To ensure that the spudcan has sufficient capacity, reliable solutions for predicting the bearing capacity of spudcans are significant

***Corresponding author:** suraparb@hotmail.com
doi: 10.14456/scitechasia.2022.35

in the design process. An overview of the mobile-drilling jack-up platform can be found in the book by Randolph and Gourvenec [1].

By using the method of characteristics (MoC), Cassidy and Houlsby [2] and Houlsby and Martin [3] presented plastic solutions of the bearing capacity factors of conical footings in sand and clay, respectively. The finite element limit analysis (FELA) was employed by Khatri and Kumar [4] and Chakraborty and Kumar [5] to derive the ultimate vertical load of conical footings in cohesionless soil. Later, Chakraborty and Kumar [6] also used FELA to compute the bearing capacity factors of conical footings in cohesive-frictional soil. However, these previous studies were limited to the cases of isotropic soils obeying the Mohr-Coulomb failure criterion.

It is widely known that natural clays exhibit some degree of strength anisotropy since the processes of soil deposition and sedimentation can cause a preferred particle orientation and stress-induced anisotropy. As a result, the strengths of soft clays significantly depend on the orientation of depositional direction. Ladd [7] and Ladd and Degroot [8] discovered that the anisotropic undrained shear strengths are a function of the plasticity index (PI) of clays, where the anisotropic undrained shear strengths are acquired from triaxial compression, triaxial extension, and direct simple shear. Note that the notations of these three anisotropic undrained shear strengths are symbolized by S_{uc} (for compression), S_{ue} (for extension), and S_{us} (for simple shear). In the past, failure criteria of anisotropic clays have been developed by some researchers such as Su et al. [10], Davis and Christian [11], and Keawsawasvong and Ukritchon [12]. These previously proposed failure criteria have been employed to study several stability problems in the past [13-16]. Recently, Krabbenhøft et al. [17] presented the AUS (anisotropic undrained shear strength) failure criterion that can efficiently capture various aspects of undrained shear strengths of anisotropic clays, which was very recently employed by Keawsawasvong and Lawongkerd [18] to derive the numerical solutions of pullout capacity of planar caissons in anisotropic clays. In addition, Yodsomjai et al. [19] also applied the AUS failure criterion to solve the stability solutions of unsupported conical slopes in anisotropic clays.

All previous studies concern the bearing capacity factor of spudcans in isotropic soil. The study on the same problem in anisotropic soil has never received attention in the past. This paper aims to present new plastic solutions of the bearing capacity factor of spudcans in anisotropic clay obeying the AUS failure criterion introduced by Krabbenhøft et al. [17]. The results are numerically derived by employing the lower bound (LB) and upper bound (UB) finite element limit analysis (FELA) to perform the numerical computation. Note that the FELA [20] is a computational method that combines the theorem of classical plasticity, the technique of numerical discretization using finite element, and mathematical optimization. Thus, this FELA has been now employed to accurately compute several stability problems and also used to obtain the numerical solutions of the bearing capacity factor of spuncans in anisotropic clay in this study. The details of practical methods to find anisotropic parameters can be found in Ratananikom et al. [21-22].

2. Problem Definition

The problem definition and notation of a spudcan are expressed in Fig. 1, where R and β represents the spudcan radius and the cone apex angle, respectively. The problem is under axisymmetric conditions owing to its conical shape. The total vertical force applied to the spudcan is symbolized by V as shown in Fig. 1. The uniformed

pressure denoted as q has a relation with V and R and can be written as:

$$q = \frac{V}{\pi R^2}. \tag{2.1}$$

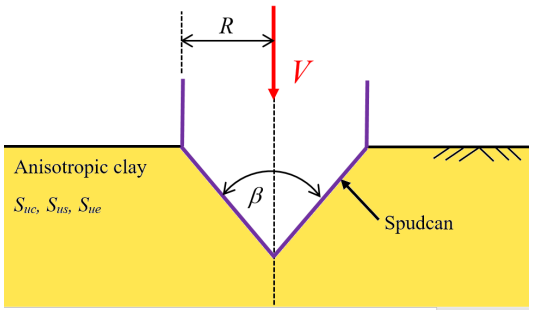

Fig. 1. Problem definition of a spudcan in anisotropic clay.

For the strengths of an anisotropic clay based on the AUS failure criterion, the clay has three anisotropic undrained shear strengths acquired from triaxial compression (S_{uc}), triaxial extension (S_{ue}), and direct simple shear (S_{us}) as mentioned in Section 1. In this study, only the effect of these anisotropic strengths is investigated. Hence, the unit weight of clay is set to be zero in order to neglect the influence of the unit weight that can disturb computed results. The interface condition at the contact surface between the spudcan and the clay is fully rough.

Ladd [7] and Ladd and Degroot [8] proposed that the degree of undrained strength anisotropy of clays can be expressed as two main strength ratios which are denoted by r_e and r_s as expressed in Eqs. (2.2) and (2.3), respectively.

$$r_e = \frac{S_{ue}}{S_{uc}}, \tag{2.2}$$

$$r_s = \frac{S_{us}}{S_{uc}}. \tag{2.3}$$

From the above equations, r_e and r_s are a function of three anisotropic shear strengths including S_{uc}, S_{ue}, and S_{us}. Ladd [7] and Ladd and Degroot [8] also pointed out that the value of S_{us} seems to be slightly lower than the average value of S_{uc} and S_{ue}. Thus, an essential assumption relating to the relationship of S_{uc}, S_{ue}, S_{us}, r_e, and r_s was also proposed by Ladd [7] and Ladd and Degroot [8] and is shown in Eqs. (2.4) and (2.5).

$$S_{us} = \frac{2S_{ue}S_{uc}}{(S_{uc} + S_{ue})}, \tag{2.4}$$

$$r_s = \frac{2r_e}{1 + r_e}. \tag{2.5}$$

Hereafter, the value of S_{us} is set to depend on the values of S_{uc} and S_{ue} according to Eq. (2.4). As a result, the r_s ratio is also described as a function of the r_e ratio as expressed in Eq. (2.5). From Eqs. (2.4) and (2.5), by setting $r_e = 1$ and $r_s = 1$ corresponding to the case of $S_{uc} = S_{ue} = S_{us}$, the AUS failure criterion becomes the Tresca failure criterion (or the Mohr-Coulomb failure criterion without the consideration of the friction angle ϕ).

By using the dimensionless technique [23-24], totally five non-dimensionless parameters including q, R, S_{uc}, S_{ue}, and β are then reduced to be three dimensionless parameters as follows:

$$\frac{q}{S_{uc}} = f(\beta, r_e), \tag{2.6}$$

where q/S_{uc} denotes the bearing capacity factor; β represents the cone apex angle; r_e corresponds to the undrained shear strength ratio obtained from triaxial compression (S_{uc}) and triaxial extension (S_{ue}).

3. Method of Analysis

This paper applied the powerful technique of UB and LB FELA to derive the numerical solutions of a spudcan in anisotropic clay by using the commercial

software, namely OptumG2 [25]. The problem of a spudcan is in axisymmetric conditions. As a result, to simulate the model of this problem, only half of the domain is modeled in OptumG2. Examples of the models for the cases of $\beta = 30°$, 90°, and 180° are shown in Figs. 2(a), 2(b), and 2(c), respectively.

Perfectly rigid elements are employed to model the spudcan. For the anisotropic clay, elements with the rigid-plastic material with the associated flow rule that obeys the AUS failure criterion [17] are applied. As mentioned earlier, the input strength parameters for the AUS model in OptumG2 are only S_{uc} and r_e, where r_s is strictly set to be a function of r_e as shown in Eq. (2.5). The contact surface between the spudcan and the anisotropic clay is defined as the fully rough interface.

The boundary conditions of this problem are described next. At the left (symmetry plane) and the right of the domain, the roller supports are applied over the left and right planes in which only vertical movements are allowed to take place. At the bottom of the domain, the fixed supports are applied to the bottom so that there are no movements in either vertical or horizontal directions. At the top of the domain, it is a free surface everywhere except at the location that a spudcan is placed. The uniformed pressure q is vertically applied over the top of the spudcan. The integral of q over the top plane of the spudcan is the total vertical force V as described earlier in Eq. (1). At the left corner of the spudcan, a fan mesh feature is adopted to enlarge the accuracy of solutions provided by the method of FELA.

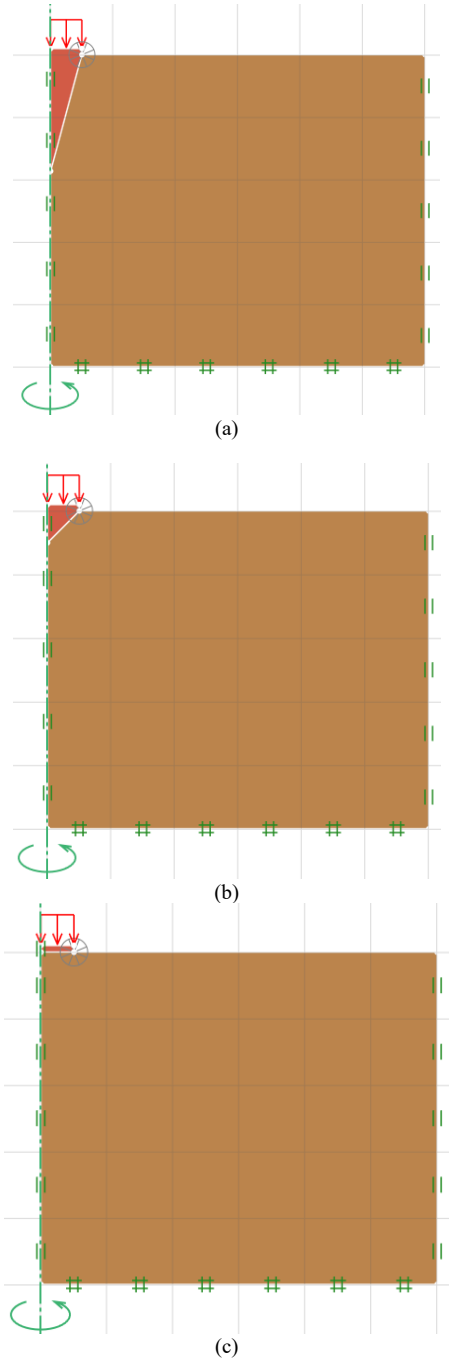

Fig. 2. A numerical model in OptumG2: (a) $\beta = 30°$, (b) $\beta = 90°$, (c) $\beta = 180°$.

The spudcan and anisotropic clay are discretized into many triangular elements. In OptumG2, LB elements are three-noded elements with linear interpolation of unknown stresses. Stress discontinuity is allowed to occur at shared edges of adjacent elements in the LB analysis. In addition, UB elements are six-noded elements that have quadratic interpolation of unknown displacements being continuous between elements. By using both LB and UB methods, the true collapse pressure q can be accurately bracketed from LB and UB solutions.

In OptumG2, there is the automatic mesh adaptivity feature that is available to be activated. This automatic mesh adaptivity is based on the technique of shear dissipation control proposed by Ciria et al. [26]. Using this feature, a number of elements considerably increase at sensitive and turbulent regions that have high plastic shear strain during the time of calculation. Krabbenhoft et al. [22], Keawsawasvong et al. [27], and Yodsomjai et al. [28] suggested that the setting of five adaptive steps of meshing with an initial mesh number of 5,000 elements that are automatically adapted and increased to a final mesh number of 10,000 elements is the suitable option for acquiring very accurate LB and UB solutions. Thus, this setting is applied to all numerical models in this study.

4. Results and Discussions

The numerical results obtained from the LB and UB FELA are first verified with the existing solutions given by Houlsby and Martin [3] for the cases of isotropic clays with the value of r_e being one. Note that, in Houlsby and Martin [3], the method of characteristics (MoC) was used to perform their solutions in which the clay is defined as a Tresca material. A comparison of bearing capacity factors between the present study (both UB and LB solutions) and Houlsby and Martin [3] (MoC solutions) is shown in Fig. 3. It can be seen from Fig. 3 that the present UB and LB solutions are slightly lower than those of Houlsby and Martin [3]. It is due to the failure criterion used in the present study is the AUS model while that of Houlsby and Martin [3] is the Tresca model.

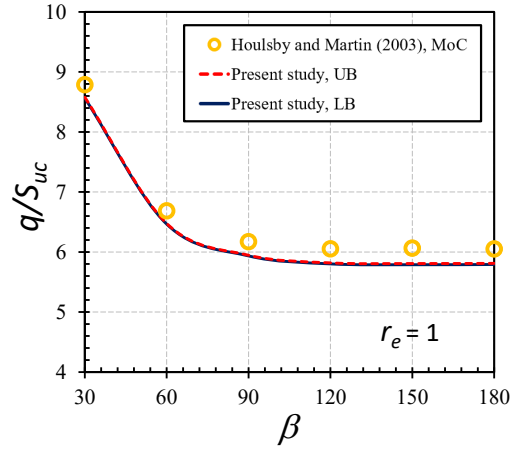

Fig. 3. A comparison of bearing capacity factors of spudcans in anisotropic clay with $r_e = 1$.

The solutions of the bearing capacity factors are presented in Figs. 4 and 5 to portray the impacts of the cone apex angle β and the undrained shear strength ratio r_e, respectively. Note that, in all cases, the exact bearing capacity factors q/S_{uc} can be accurately bracketed within 1% difference between the LB and UB solutions. The relationship between the bearing capacity factors q/S_{uc} and the cone apex angle β is shown in Fig. 4 for different values of the undrained shear strength ratio r_e. It can be clearly seen that the relationship between q/S_{uc} and β is nonlinear. An increase in β causes a decrease in q/S_{uc}. The values of q/S_{uc} become almost constant when the values of β become larger than 120°. This implies that the impact of β on q/S_{uc} becomes insignificant when the values of β > 120°. Fig. 5 demonstrates the relationship between q/S_{uc} and r_e for the different values of β. Since the q/S_{uc} values for the cases of β = 150° and 180° are equal, only the cases of β = 150° are shown in Fig. 5. The nonlinear

relationship between q/S_{uc} and r_e can be observed, where an increase in r_e results in an increase in q/S_{uc}. The presented solutions of the bearing capacity factors for spudcans in anisotropic clays can be used by geotechnical engineers to predict the ultimate vertical force of spudcan foundations for several offshore structures.

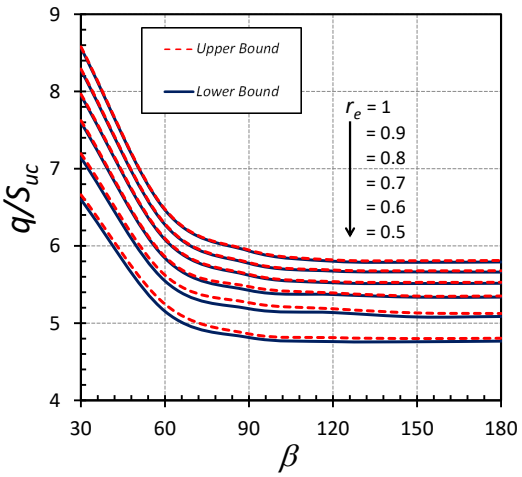

Fig. 4. Relationship between q/S_{uc} and β (°).

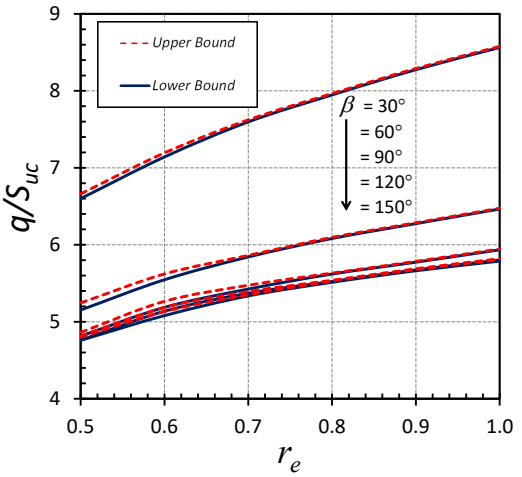

Fig. 5. Relationship between q/S_{uc} and r_e.

5. Failure Mechanisms

The impacts of β and r_e on the failure mechanisms of spudcans in anisotropic clays are investigated in Figs. 6-7 (for β) and Figs. 8-9 (for r_e). Figs. 6 and 7 present the influence of β on the failure mechanism including the final adaptive meshes and the incremental shear strain contours, respectively, for the cases of r_e = 0.7 and β = 30°, 90°, and 180°. From Fig. 6, it is evident that a number of elements significantly increase at sensitive and turbulent regions that can reveal high plastic shear zones. This results in an increase in the accuracy of the computed numerical results shown in Figs. 4 and 5. It can be observed from Figs. 6 and 7 that the sizes of the failure mechanisms of spudcans significantly decrease as the values of β decrease in both vertical and horizontal directions. The size of the failure mechanism for the extreme case with β = 30° is about 4R in both horizontal and vertical direction whereas those of the cases of β = 90° and 180° are about 2.5R in the horizontal direction and 1.5 R in the vertical direction. Figs. 8 and 9 present the influence of r_e on the failure mechanism including the final adaptive meshes and the incremental shear strain contours, respectively, for the cases of β = 60° and r_e = 0.5, 0.7, and 1. It is found in Figs. 8 and 9 that the impact of r_e on the failure mechanisms is quite small. When the values of r_e increase, the sizes of the failure mechanisms become slightly smaller. In Figs. 8 and 9, the size of the failure mechanism of the extreme case with r_e = 0.5 is approximately 3.5R in horizontal direction and 2.1R in vertical direction. The sizes of the failure mechanisms of other cases are a little smaller than the extreme case as can be seen in Figs. 8 and 9. However, the impact of r_e on the bearing capacity factor is significant as demonstrated in Fig. 5.

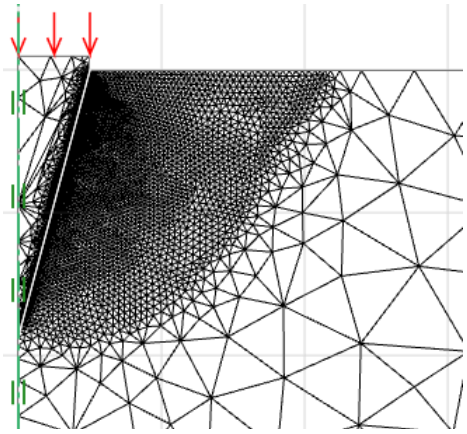

(a)

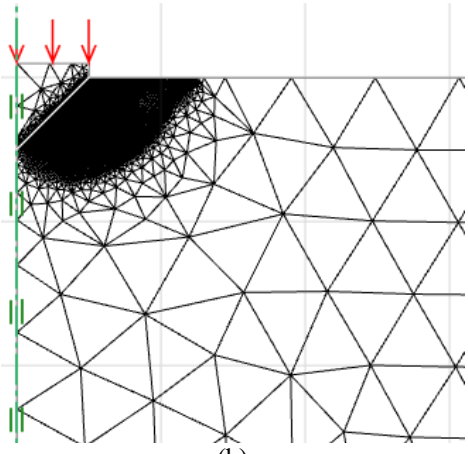

(b)

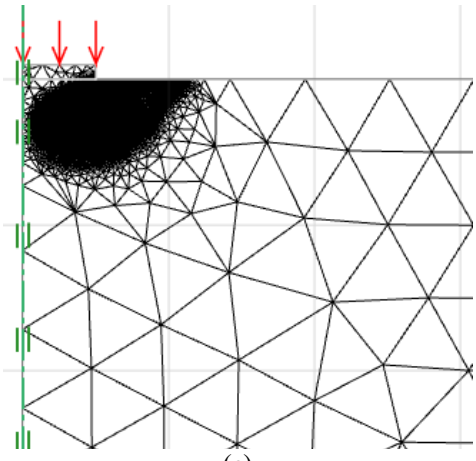

(c)

Fig. 6. Effect of β on the final adaptive meshes of spudcans in anisotropic clay with $r_e = 0.7$: (a) $\beta = 30°$, (b) $\beta = 90°$, (c) $\beta = 180°$.

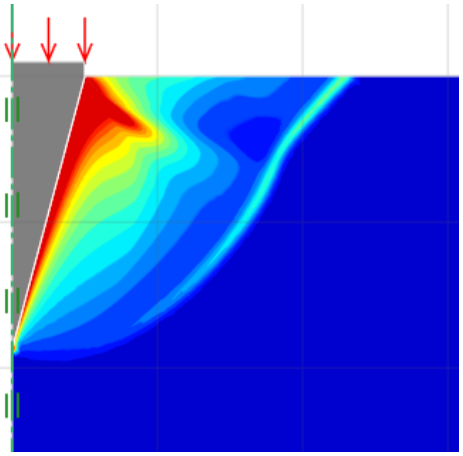

(a)

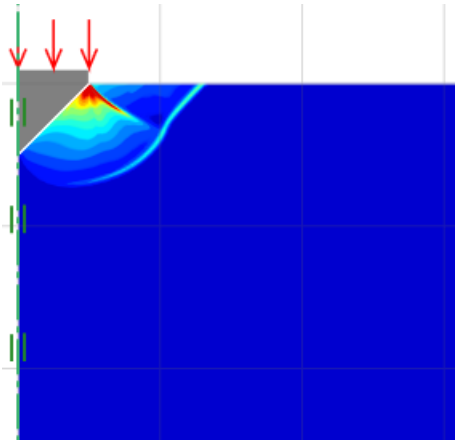

(b)

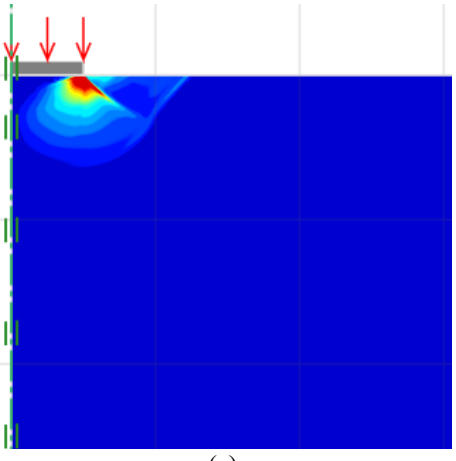

(c)

Fig. 7. Effect of β on the incremental shear strain contours of spudcans in anisotropic clay with $r_e = 0.7$: (a) $\beta = 30°$, (b) $\beta = 90°$, (c) $\beta = 180°$.

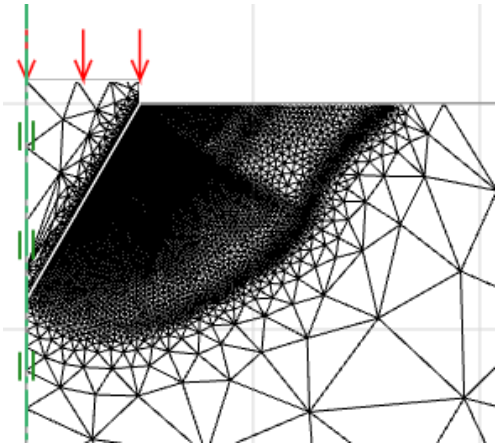

(a)

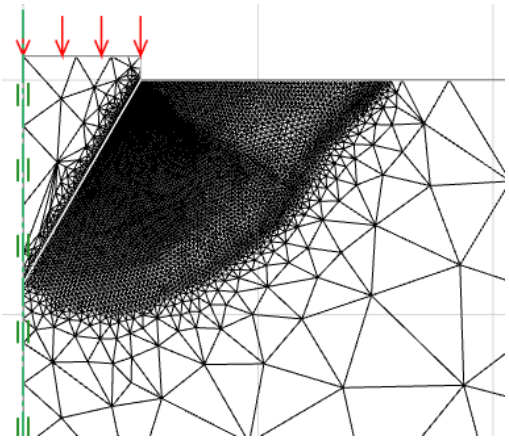

(b)

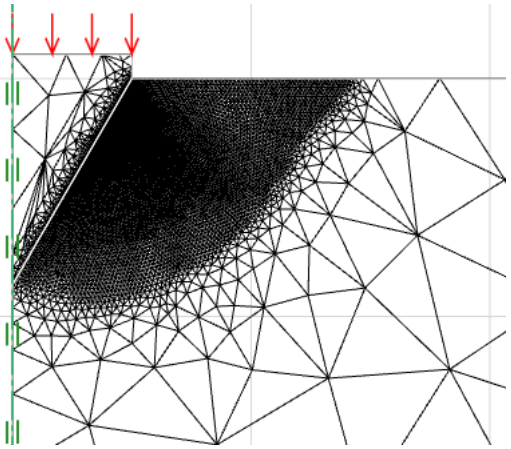

(c)

Fig. 8. Effect of r_e on the final adaptive meshes of spudcans in anisotropic clay with $\beta = 60°$: (a) $r_e = 0.5$, (b) $r_e = 0.7$, (c) $r_e = 1.0$.

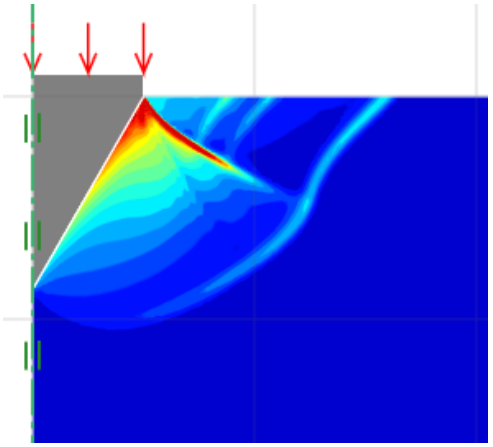

(a)

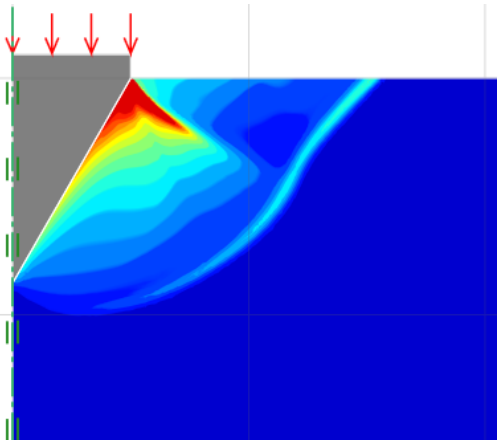

(b)

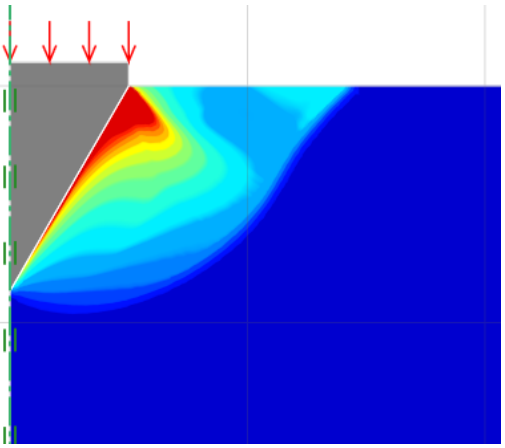

(c)

Fig. 9. Effect of r_e on the incremental shear strain contours of spudcans in anisotropic clay with $\beta = 60°$: (a) $r_e = 0.5$, (b) $r_e = 0.7$, (c) $r_e = 1.0$.

6. Conclusion

This paper demonstrates the influence of anisotropic undrained shear strengths of soft clays as well as the foundation shapes on the ultimate bearing capacity of spudcans in anisotropic clays. The UB and LB FELA techniques are employed to compute the bearing capacity factor of the particular problem. In this study, the anisotropic clay is governed by the AUS failure criterion that has three anisotropic undrained shear strengths obtained from triaxial compression, triaxial extension, and direct simple shear. These anisotropic undrained shear strengths are reduced in the form of the undrained shear strength ratio. In this paper, two dimensionless parameters include the cone apex angle and the undrained shear strength ratio. Influences of these dimensionless parameters on the bearing capacity factors and the failure mechanisms are investigated. The design charts for this problem are also proposed for general design purposes.

References

[1] Randolph M, Gourvence S. Offshore geotechnical engineering. Spon Press: Taylor & Francis; 2011.

[2] Cassidy MJ, Houlsby GT. Vertical bearing capacity factors for conical footings on sand. Géotechnique 2002;52(9):687-92.

[3] Houlsby GT, Martin CM. Undrained bearing capacity factors for conical footings on clay. Géotechnique 2003;53(5):513-20.

[4] Khatri VN, Kumar J. Bearing capacity factor Nγ for a rough conical footing. Geomech Eng 2009;1(3):205-18.

[5] Chakraborty D, Kumar J. The size effect of a conical footing on Nγ. Comput Geotech 2016;76:212-21.

[6] Chakraborty M, Kumar J. (2015) Bearing capacity factors for a conical footing using lower- and upper-bound finite elements limit analysis. Can Geotech J 2015;52:1-7.

[7] Ladd CC. Stability evaluations during stage construction. J Geotech Eng 1919;117(4):540-615.

[8] Ladd CC, DeGroot DJ. Recommended practice for soft ground site characterization. In Proc 12th Panamerican Conference on Soil Mechanics and Geotechnical Engineering, Cambridge; 2003.

[9] Davis EH, Christian JT. Bearing capacity of anisotropic cohesive soil. J Soil Mech Found Div 1971;97(5):753-69.

[10] Su SF, Liao HJ, Lin YH. Base stability of deep excavation in anisotropic soft clay. J Geotech Geoenviron Eng 1998;124(9): 809-19.

[11] Davis EH, Christian JT. Bearing capacity of anisotropic cohesive soil. J Soil Mech Found Div. 1971;97(5):753-69.

[12] Ukritchon B, Keawsawasvong S. Three-dimensional lower bound finite element limit analysis of an anisotropic undrained strength criterion using second-order cone programming. Comput Geotech 2019;106:327-44.

[13] Ukritchon B, Keawsawasvong S. Lower bound limit analysis of an anisotropic undrained strength criterion using second-order cone programming. Int J Numer Anal Methods Geomech 2018;42(8):1016-33.

[14] Ukritchon B, Keawsawasvong S. Undrained lower bound solutions for end bearing capacity of shallow circular piles in non-homogeneous and anisotropic clays. Int J Numer Anal Methods Geomech 2020;44(5):596-632.

[15] Ukritchon B, Keawsawasvong S. Lower bound solutions for undrained face stability of plane strain tunnel headings in

anisotropic and non-homogeneous clays. Comput Geotech 2019;112:204-17.

[16] Ukritchon B, Keawsawasvong S. Undrained stability of unlined square tunnels in clays with linearly increasing anisotropic shear strength. Geotech Geol Eng 2020;38(1):897-915.

[17] Krabbenhøft K, Galindo-Torres SA, Zhang X, Krabbenhøft J. AUS: Anisotropic undrained shear strength model for clays. Int J Numer Anal Methods Geomech 2019;43(17):2652-66.

[18] Keawsawasvong S, Lawongkerd J. Influences of anisotropic undrained shear strengths of clays on pullout capacity of planar caissons Science & Technology Asia 2021.

[19] Yodsomjai W, Keawsawasvong S, Senjuntichai T. Undrained stability of unsupported conical slopes in anisotropic clays based on AUS failure criterion. Transp Infrastruct Geotech 2021.

[20] Sloan SW. Geotechnical stability analysis. Géotechnique 2013;63(7):531-72.

[21] Ratananikom W, Likitlersuang S, Yimsiri S. An investigation of anisotropic elastic parameters of Bangkok clay from vertical and horizontal cut specimens. Geomech Geoeng 2013;8(1):15-27.

[22] Ratananikom W, Yimsiri S, Fukuda F, Likitlersuang S. Undrained strength-deformation characteristics of Bangkok Clay under general stress condition. Geomech Eng 2013;5(5):419-45.

[23] Butterfield R. Dimensional analysis for geotechnical engineering. Géotechnique 1999;49(2):357-66.

[24] Keawsawasvong S, Likitlersuang S. Undrained stability of active trapdoors in two-layered clays. Underground Space 2020.

[25] Krabbenhoft K, Lyamin A, Krabbenhoft J. Optum computational engineering (OptumG2) [cited 2020 Feb 01]. Available from: http://www.optumce.com

[26] Ciria H, Peraire J, Bonet J. Mesh adaptive computation of upper and lower bounds in limit analysis. Int J Numer Met in Eng 2008;75:899-944.

[27] Keawsawasvong, S, Thongchom C, Likitlersuang S. Bearing capacity of strip footing on Hoek-Brown rock mass subjected to eccentric and inclined loading. Transportation Infrastructure Geotechnology 2020.

[28] Yodsomjai W, Keawsawasvong S, Likitlersuang S. Stability of unsupported conical slopes in Hoek-Brown rock masses. Transportation Infrastructure Geotechnology 2020.